ACS Infectious Diseases

Letter

Cite This: ACS Infect. Dis. 2018, 4, 1540−1545

pubs.acs.org/journal/aidcbc

# Discovery and Optimization of nTZDpa as an Antibiotic Effective Against Bacterial Persisters

Wooseong Kim,[†] Andrew D. Steele,[‡] Wenpeng Zhu,[§] Erika E. Csatary,[‡] Nico Fricke,[§] Madeline M. Dekarske,[‡] Elamparithi Jayamani,[†] Wen Pan,[†] Bumsup Kwon,[▽] Isabelle F. Sinitsa,[∥] Jake L. Rosen,[‡] Annie L. Conery,[#,○] Beth Burgwyn Fuchs,[†] Petia M. Vlahovska,[⊥] Frederick M. Ausubel,[#,○] Huajian Gao,[§] William M. Wuest,*[,‡] and Eleftherios Mylonakis*[,†]

[†]Division of Infectious Diseases, Rhode Island Hospital and Warren Alpert Medical School of Brown University, 593 Eddy Street, Providence, Rhode Island 02903, United States

[‡]Department of Chemistry and Emory Antibiotic Resistance Center, Emory University, 1515 Dickey Drive, Atlanta, Georgia 30322, United States

[§]School of Engineering, Brown University, 184 Hope Street, Providence, Rhode Island 02903, United States

[▽]Division of Neurology, Rhode Island Hospital and Warren Alpert Medical School of Brown University, 593 Eddy Street, Providence, Rhode Island 02903, United States

[∥]Department of Chemistry, Temple University, 1901 N. 13th Street, Philadelphia, Pennsylvania 19122, United States

[#]Department of Molecular Biology, Massachusetts General Hospital, 185 Cambridge Street, Boston, Massachusetts 02115, United States

[○]Department of Genetics, Harvard Medical School, 185 Cambridge Street, Boston, Massachusetts 02115, United States

[⊥]Department of Engineering Sciences and Applied Mathematics, Northwestern University, 2145 Sheridan Road, Evanston, Illinois 60208, United States

Supporting Information

**ABSTRACT:** Conventional antibiotics are not effective in treating infections caused by drug-resistant or persistent nongrowing bacteria, creating a dire need for the development of new antibiotics. We report that the small molecule nTZDpa, previously characterized as a nonthiazolidinedione peroxisome proliferator-activated receptor gamma partial agonist, kills both growing and persistent *Staphylococcus aureus* cells by lipid bilayer disruption. *S. aureus* exhibited no detectable development of resistance to nTZDpa, and the compound acted synergistically with aminoglycosides. We improved both the potency and selectivity of nTZDpa against MRSA membranes compared to mammalian membranes by leveraging synthetic chemistry guided by molecular dynamics simulations. These studies provide key insights into the design of selective and potent membrane-active antibiotics effective against bacterial persisters.

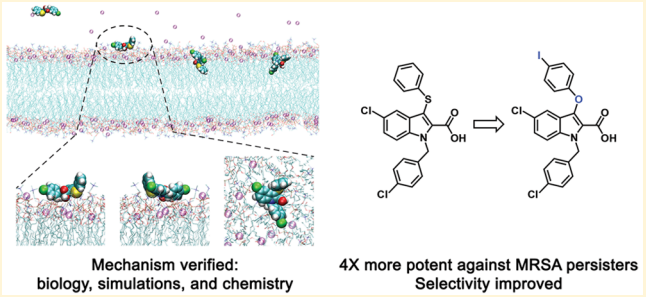


**KEYWORDS:** *MRSA, persisters, antibiotics, membrane-active agent, MD simulations, SAR*

*Staphylococcus aureus* is a leading cause of both hospital and community-acquired infections, causing a wide range of diseases from mild skin abscesses to life-threatening infections.[1] The failure of antibiotic therapy against *S. aureus* is associated with both multidrug resistant strains[2] and its ability to adopt a dormant so-called persister lifestyle.[3] Persisters tolerate high concentrations of conventional antibiotics[4−7] due to their nongrowing dormant state in which biosynthetic processes targeted by conventional antibiotics are inactive or significantly attenuated.[3] Persisters are responsible for the antibiotic tolerance of biofilms and the recalcitrance of chronic infections.[3,8,9]

We previously reported an automated high-throughput screen to identify compounds that rescue *Caenorhabditis elegans* from MRSA infections[10] that excludes compounds that are toxic to *C. elegans*.[11] Among ∼82 000 compounds screened, we showed that one lead compound, the synthetic retinoid CD437, kills MRSA persisters by membrane disruption.[12] Subsequent synthetic chemical optimization identified an analog more selective for bacterial membranes.[12] In this paper, we describe the optimization of another membrane-active compound,

**Received:** July 6, 2018
**Published:** August 22, 2018






DOI: 10.1021/acsinfecdis.8b00161
ACS Infect. Dis. 2018, 4, 1540−1545

nTZDpa (**1**, Scheme 1), a nonthiazolidinedione peroxisome proliferator-activated receptor gamma (PPAR$\gamma$) partial agonist that has been investigated *in vivo* for diabetes therapy.[13]

**Scheme 1. Synthesis of nTZDpa and Main Discoveries from Our First-Generation Synthetic Studies**

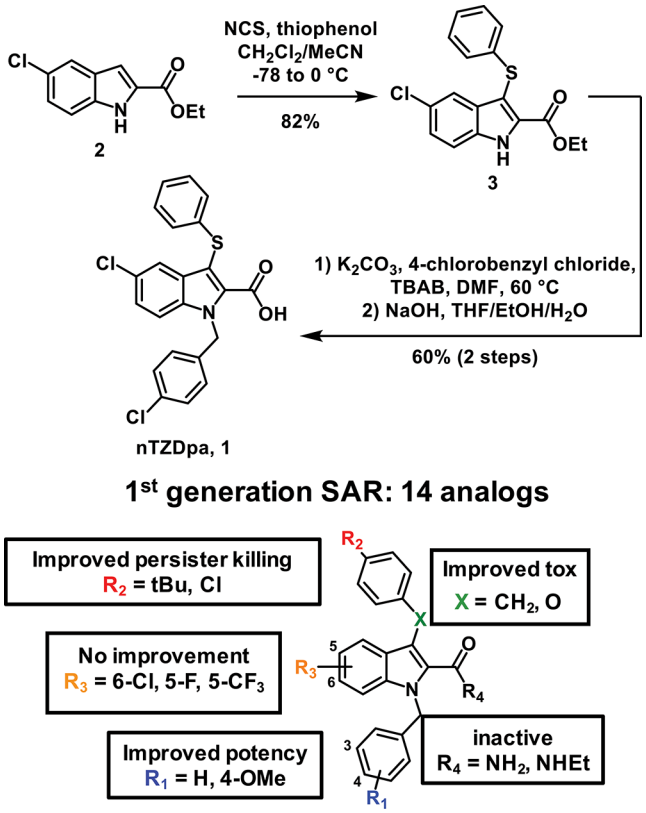


nTZDpa rescued ~90% of *C. elegans* from MRSA-mediated lethality with an $EC_{50}$ (median effective concentration) of ~0.6 $\mu$g/mL (Figure 1A). *In vitro* nTZDpa exhibited antimicrobial activity against a panel of both *S. aureus* and *Enterococcus faecium* clinical strains, including the multidrug-resistant *S. aureus* strain VRS1, with a minimal inhibitory concentration (MIC) of ~4 $\mu$g/mL (Table S1). nTZDpa acted synergistically with aminoglycosides (gentamicin, tobramycin, neomycin, kanamycin, and streptomycin) with a fractional inhibitory concentration index of $\leq$0.5 but not with vancomycin, ciprofloxacin, rifampicin, or tetracycline (Figure S1). nTZDpa was not effective against Gram-negative bacteria (Table S1).

Unexpectedly, 16 $\mu$g/mL nTZDpa completely eradicated ~$10^7$ CFU/mL exponential-phase MRSA MW2 within 2 h, which was similar to 32 $\mu$g/mL gentamicin and faster than 32 $\mu$g/mL ciprofloxacin or 32 $\mu$g/mL vancomycin (Figure S2A). Further, nTZDpa exhibited extremely low probabilities of resistance development (Figure 1B). Whereas MRSA MW2 showed a 32-fold higher MIC to ciprofloxacin than wild-type after 25 days of serial passage in sub-MIC concentrations, MW2 did not acquire resistance to nTZDpa (Figure 1B).

Notably, nTZDpa was also potent against MRSA persisters. High concentrations of conventional antibiotics had no effect on the viability of MRSA persisters (Figure S2B), whereas nTZDpa caused an ~2-log reduction at 32 $\mu$g/mL and completely eradicated ~$5 \times 10^7$ CFU/mL persisters within 2 h at 64 $\mu$g/mL (Figure 1C). nTZDpa also exhibited synergistic bactericidal activity with aminoglycosides against both stationary-phase and biofilm MRSA persisters (Figures 1C and S2C,D).

Our findings that nTZDpa exhibits fast-killing rates, low probabilities of resistance, bactericidal activity against persister cells, and synergism with aminoglycosides are consistent with the possibility that nTZDpa is a membrane-active compound.[10,11] Indeed, transmission electron micrographs of MRSA cells treated with nTZDpa showed mesosome formation, abnormal cell division, and cell lysis (Figure 2A). Further, nTZDpa induced membrane permeabilization of MRSA cells (Figure 2B) and disrupted *S. aureus* biomembrane-mimicking giant unilamellar vesicles (7:3 DOPC/DOPG, 1,2-dioleoyl-*sn*-glycero-3-phosphocholine/glycerol, Figure 2C and Videos S1 and S2).[12] These results demonstrate that nTZDpa disrupts the physical integrity of the cell membranes rather than targeting membrane proton motive force (PMF) because ionophores dissipating PMF do not induce SYTOX Green membrane permeability or the killing of MRSA persisters.[12]

Membrane active agents are typically toxic to mammalian cells.[10] Although nTZDpa did not induce significant hemolysis of human erythrocytes at or below 16 $\mu$g/mL, we observed significant hemolysis above this threshold (Figure 1D). The observed hemolytic activity of nTZDpa at high concentrations was reflected by its toxicity toward two mammalian cell lines at 32 $\mu$g/mL (HepG2 and HKC-8, Figure S2E).

The potential deficits of nTZDpa as an antibiotic are its relatively high MICs of 4 and 64 $\mu$g/mL for *S. aureus* growing and persister cells, respectively, and relatively low membrane selectivity. To improve both the potency and selectivity of nTZDpa, we first carried out molecular dynamics (MD) simulations, which demonstrated that nTZDpa interacts with the membrane surface via the carboxylic acid moiety and two chlorine atoms that bind strongly to hydrophilic lipid heads (Figure 2D, Video S3). These contacts enable nTZDpa to overcome the energy barrier for penetration into the outer leaflet of the membrane via hydrophobic interactions between its aromatic rings and the hydrophobic tails of membrane lipids (Figure 2D, Video S3). Figure 2E shows that membrane penetration of nTZDpa involves a transfer energy of $-0.81\ k_BT$ and an energy barrier of $6.14\ k_BT$ (Figure 2E, Table S2), suggesting that the membrane penetration of nTZDpa is spontaneous and rapid at ambient temperature.[14,15] At equilibrium, nTZDpa molecules are embedded in the outer leaflet of the membrane with an inclined orientation with respect to the acyl chains of lipids (Figures 2D and S3). These simulations led us to ask four questions: (1) Is the acid essential for initial attachment? (2) Would movement, removal, or replacement of chlorine on the indole or the benzyl substituent improve activity? (3) Could additional substituents on the unchlorinated phenyl group improve activity? (4) Could substitution of sulfur with a different atom/functionality improve activity?

With these questions in mind, we designed a concise synthesis of nTZDpa amenable to analog development (Scheme 1). We synthesized amide derivatives **S1** and **S2** to test the importance of the carboxylic acid moiety ($R^4 = NH_2$, NHEt, Scheme 1), as well as a truncated *N*-methyl derivative **S3** to probe the necessity of the benzyl substituent (Figure S4). None of these three compounds showed significant antibiotic activity (MIC $\geq$ 64 $\mu$g/mL) or induced membrane permeabilization (Figure S5). MD simulations with amide analog **S1** (Figure 2E, Video S4) showed that it could approach, but not penetrate, the membrane due to electrostatic repulsion between the nitrogen atom of the


DOI: 10.1021/acsinfecdis.8b00161
ACS Infect. Dis. 2018, 4, 1540−1545

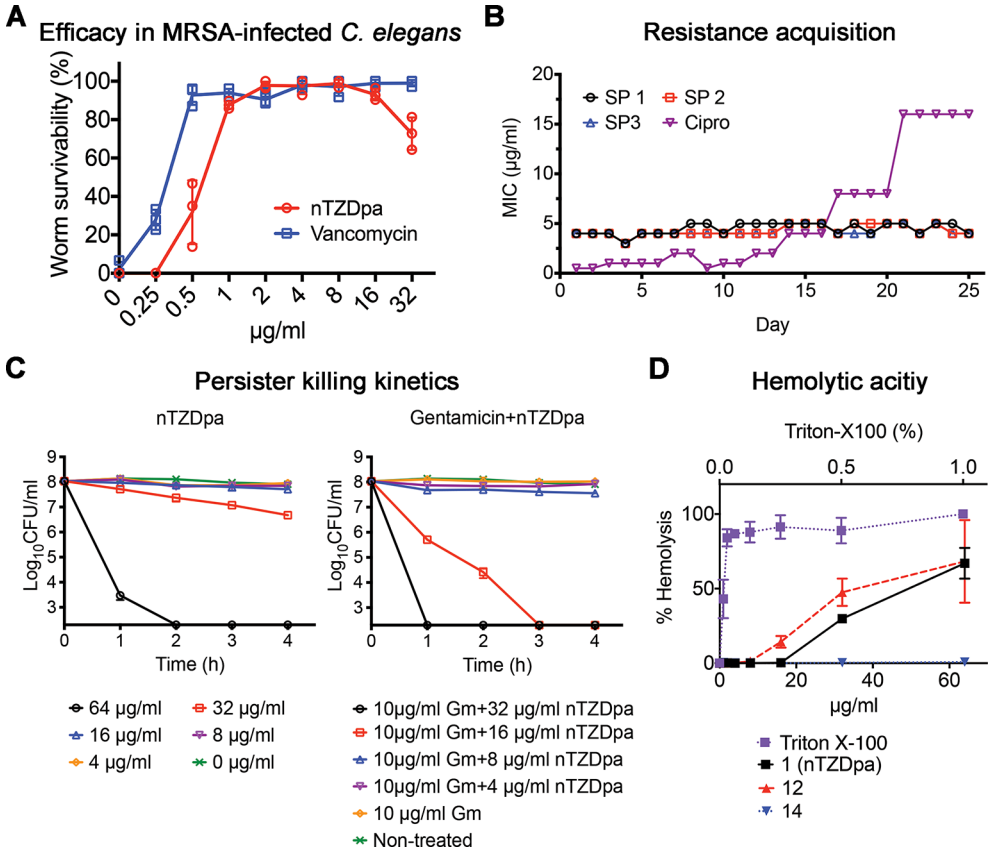


**Figure 1.** (A) Dose-dependent *C. elegans* survival from MRSA infections in the presence of nTZDpa and vancomycin. (B) Three attempts to develop MRSA resistance to nTZDpa (SP 1, 2, and 3) and to ciprofloxacin over 25 days. (C) Time-dependent killing of MRSA persister cells by nTZDpa and nTZDpa/gentamicin combinations. (D) Hemolysis assay with human erythrocytes using 1% Triton X-100 as a positive control (**12** and **14** refer to the compounds in Table 1). (A, C, D) Error bars denote s.d. ($n$ = 3).

amide and the negatively charged membranes (details in SI Results, Figures 2E and S6−S8, Videos S4 and S5).

A series of analogs (Figure S4) showed that the chlorine substituent on the benzyl moiety ($R^1$, Scheme 1) is important for activity. Removal resulted in less potency against growing MRSA and less toxicity (Figures 2E and S4, and S5). The position of chlorine on the benzyl moiety did not seem to be important, however, as placement on 4- or 3-position had minimal effects on potency and selectivity (Figures S4 and S5).

We also investigated substituents at $R^2$ of the arylthioether (Scheme 1). The addition of either a *tert*-butyl or chlorine substituent resulted in increased potency against both planktonic and persister cells (Figures S4 and S5) but increased toxicity (compare **4** and **5**, Table 1). Next, we probed substitution of the indole ring ($R^3$, Scheme 1). None of these changes resulted in improved biological activity.

Importantly, MD simulations were consistent with the potency data. Experimentally, the loss of one chlorine (**S4**) resulted in reduced antimicrobial activity and membrane permeability (Figures S4 and S5), which was reflected in the MD simulations, which showed that **S4** exhibited an increased transfer energy of −0.27 $k_BT$ and an energy barrier of 17.98 $k_BT$ relative to nTZDpa (Figure 2E, Table S2, Video S6). Similarly, an additional chlorine (**4**) resulted in increased potency against both planktonic and persister cells (Figures S4, S5, and S9) and a much lower transfer energy of −13.62 $k_BT$ and energy barrier of 0.79 $k_BT$, compared to nTZDpa (Figure 2E, Table S2, Video S7).

The nTZDpa MD simulations showed that the sulfur atom interacts with the membrane early in the attachment phase (Figure 2D, $t$ = 180 ns, front view). Substitution of the sulfur with methylene (**S12**, Figure S4) resulted in less potency, but replacement with oxygen yielded an analog that was equipotent with nTZDpa for growing *S. aureus* cells but showed improved membrane selectivity and cytotoxicity profiles (**6**, Table 1 and Figure S2E). Unfortunately, a major drawback of compound **6** is that treatment of persisters with **6** only caused a 3-log decrease in viability at 64 μg/mL (Figure S9). Nevertheless, the increase in selectivity of analog **6** with no cost to potency against growing *S. aureus* cells led us to synthesize a second generation of nTZDpa analogs in which the sulfur was replaced with oxygen (Scheme 2).

Before we synthesized analogs with varied substituents, we synthesized the corresponding primary alcohol of **6** (**S13**), and hydrolyzed intermediate **8** to a truncated methoxy derivative (**S14**). The resultant analogs displayed a reduction/abolishment of antibiotic activity (Figure S10), which was in line with our previous results and modeling. We also varied the linker lengths between oxygen and nitrogen on the indole ring, with their corresponding aryl branch groups (see compounds **S15**−**S17**, Figure S10), all of which were less active. These data indicated that the aromatic branch groups of **6** contained the optimal spacing for activity. From here, we leveraged our synthetic route (Scheme 2) to produce 19 analogs with varied substituent patterns, similar to our first-generation approach (see Figure S10 for full list of structures and data).



DOI: 10.1021/acsinfecdis.8b00161
*ACS Infect. Dis.* 2018, 4, 1540−1545

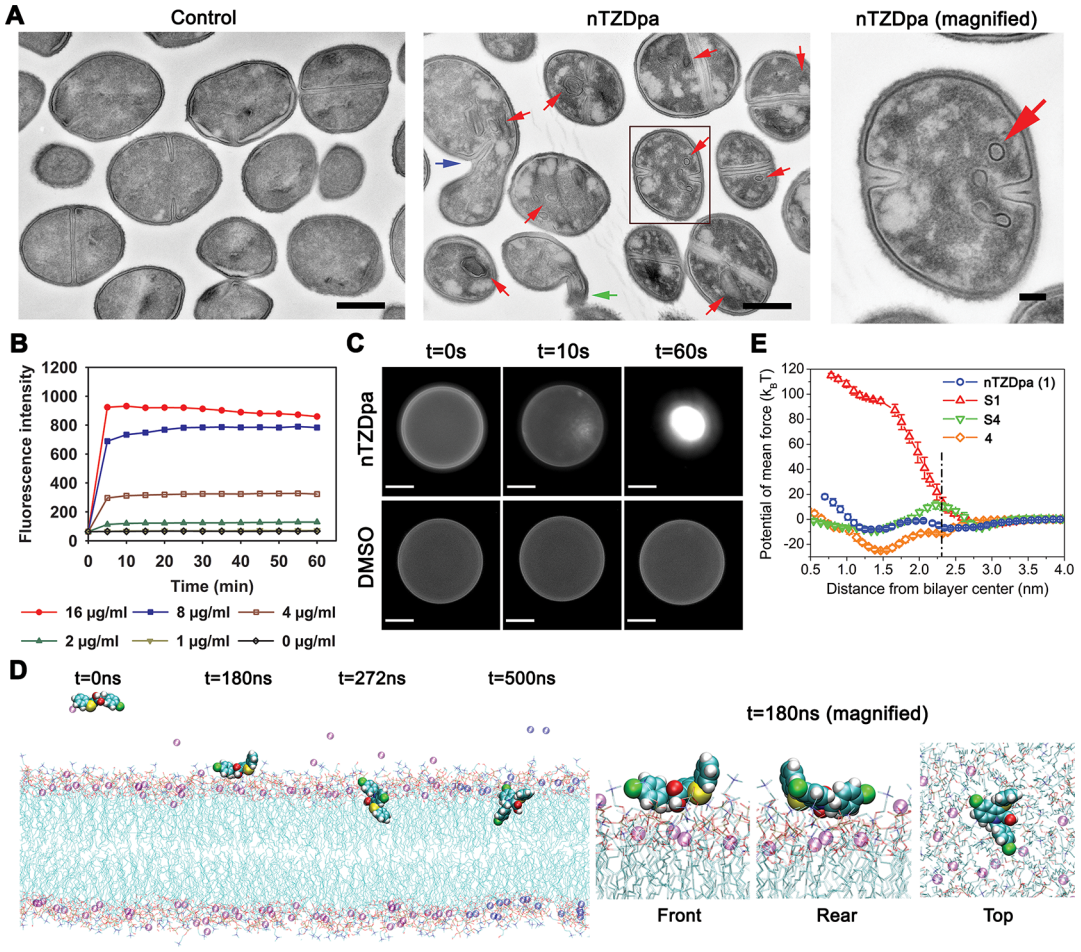


**Figure 2.** (A) TEM micrographs showing the formation of intracellular mesosome-like structures (red arrows), abnormal cell division (blue arrow), and cell lysis (green arrow) in MRSA treated with nTZDpa. Scale bars for the "control" and "nTZDpa" = 500 nm; nTZDpa (magnified) scale bar = 100 nm. (B) Membrane permeabilization of MRSA by nTZDpa monitored with SYTOX Green dye uptake. (C) GUV disruption by nTZDpa over time, with DMSO as a negative control. Scale bars = 20 $\mu$m. (D) MD simulation of nTZDpa interacting with lipid bilayer. (E) Free energy profile of nTZDpa and three analogs during MD simulations of their interactions with lipid bilayers.

**Table 1. Table of Each Major Improvement Made to nTZDpa over the Course of This Study**

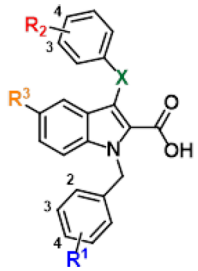

| compound[a] | $R^1$ | $R^2$ | $R^3$ | X | MIC[b] | PKC[b,c] | $HC_{50}$[b,d] |
|---|---|---|---|---|---|---|---|
| **1** (nTZDpa) | 4-Cl | H | Cl | S | 4 | 64 | 47 |
| **4** | 4-Cl | 4-Cl | Cl | S | 2 | 16 | 34 |
| **5** | 4-Cl | 4-tBu | Cl | S | 2 | 8 | 26 |
| **6** | 4-Cl | H | Cl | O | 4 | >64 | >64 |
| **10** | 3,4-Cl | H | Cl | O | 2 | 32 | >64 |
| **11** | 4-Cl | 4-Cl | Cl | O | 2 | >64 | >64 |
| **12** | 4-Cl | 3,4-Cl | Cl | O | 1 | 8 | 38 |
| **13** | 4-Cl | 4-Br | Cl | O | 2 | 32 | >64 |
| **14** | 4-Cl | 4-I | Cl | O | 1 | 16 | >64 |

[a]See the structure above the table for definitions of "R" and "X" groups. [b]Values given in $\mu$g/mL. [c]PKC: persister killing concentration to kill $5 \times 10^7$ CFU/mL MRSA persister below the limit of detection. [d]$HC_{50}$: median hemolytic concentration.

Table 1 summarizes each key improvement throughout the course of our synthetic studies. Our first-generation analogs showed that addition of a chlorine (**4**) or *tert*-butyl (**5**) substituent on the aryl thioether moiety ($R^2$, Table 1) generated more potent compounds but was not more selective for bacterial membranes. Substitution of oxygen for sulfur (**6**) improved the toxicity profile but abolished its ability to kill persisters. Our optimization of **6** showed that additional chlorine atoms on either aryl branch group (**10**, **11**, and **12**) increased potency but not selectivity. Finally, addition of bromine and especially iodine on the aryl ether moiety enhanced potency (**13**, **14**) against growing and persister cells relative to compound **6**, retaining improved membrane selectivity and cytotoxicity profiles (Figure S2E). The MD simulations suggest that larger halogens perturb the membrane more than smaller ones once penetration occurs. In addition, the decreasing polarity of halogens from chlorine to bromine to iodine increases the hydrophobic attraction between the substituent and the lipid tails upon penetration (Figure 2D, $t$ = 272 ns).

In conclusion, we discovered that nTZDpa is a potent antimicrobial that is effective against both multidrug-resistant and persistent *S. aureus*. nTZDpa kills bacteria by disrupting lipid bilayers, has a low probability of selecting for resistance, and exhibits synergism with aminoglycosides. Two rounds of



DOI: 10.1021/acsinfecdis.8b00161
*ACS Infect. Dis.* 2018, 4, 1540−1545

**Scheme 2. Synthesis of Compound 6**

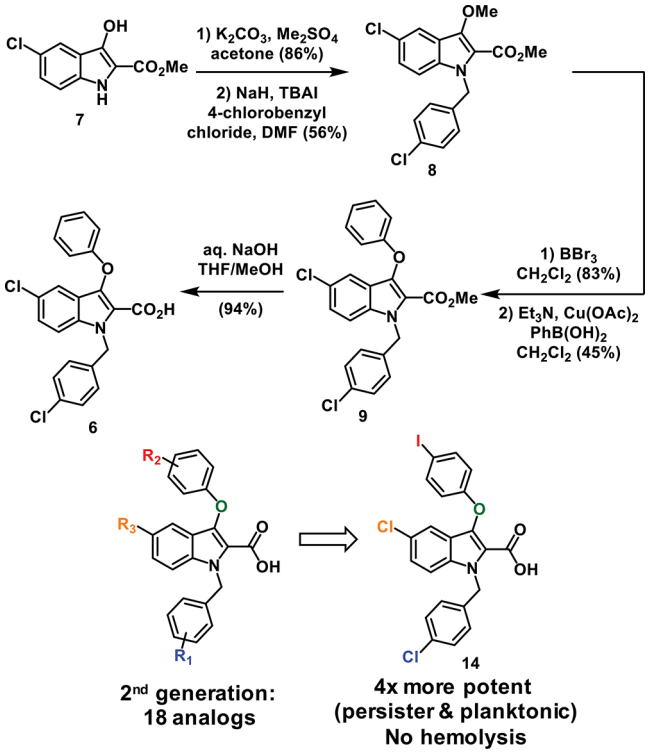


SAR optimized the substituents and the scaffold of nTZDpa to provide a more potent and selective compound (**14**). Our results provide new insights for further development and design of membrane-active antibiotics for multidrug resistant and persistent *S. aureus*.

## METHODS

Detailed experimental procedures used in this study are described in the Supporting Information.

## ASSOCIATED CONTENT

### Supporting Information

The Supporting Information is available free of charge on the ACS Publications website at DOI: 10.1021/acsinfecdis.8b00161.

Additional results, tables, figures, SI video legends, and methods (PDF)

SI Videos: nTZDpa disrupting GUVs; molecular dynamics simulation between nTZDpa or its analogs with membrane lipid bilayers (ZIP)

## AUTHOR INFORMATION

### Corresponding Authors

*E-mail: emylonakis@lifespan.org.

*E-mail: william.wuest@emory.edu.

### ORCID

Eleftherios Mylonakis: 0000-0002-4624-0777

### Notes

The authors declare the following competing financial interest(s): F.M.A. and E.M. disclose financial interests in Genma Biosciences, Inc. and Octagon Therapeutics, Inc., companies that are engaged in developing antimicrobial compounds. The remaining authors declare no competing financial interests.

## ACKNOWLEDGMENTS

This study was supported by National Institutes of Health Grant P01 AI083214 to F.M.A. and E.M., by National Science Foundation Grant CMMI-1562904 to H.G., and by National Institute of General Medical Sciences Grant 1R35GM119426 and National Science Foundation Grant NSF1755698 to W.M.W. We thank L. Rice for providing the *E. faecium* strains. MD simulations were supported by the Extreme Science and Engineering Discovery Environment through Grant MSS090046 and the Center for Computation and Visualization at Brown University.

## ABBREVIATIONS

MIC, minimum inhibitory concentration; $HC_{50}$, median hemolytic concentration; PKC, persister killing concentration to kill $5 \times 10^7$ CFU/mL MRSA persister below the limit of detection; MD, molecular dynamics; GUV, giant unilamellar vesicle; DOPC, 1,2-dioleoyl-*sn*-glycero-3-phosphocholine; DOPG, 1,2-dioleoyl-*sn*-glycero-3-phosphoglycerol; SI, selectivity index; PMF, proton motive force

## REFERENCES

(1) Tong, S. Y. C., Davis, J. S., Eichenberger, E., Holland, T. L., and Fowler, V. G. (2015) *Staphylococcus aureus* infections: epidemiology, pathophysiology, clinical manifestations, and management. *Clin. Microbiol. Rev. 28* (3), 603−661.

(2) Chambers, H. F., and DeLeo, F. R. (2009) Waves of resistance: *Staphylococcus aureus* in the antibiotic era. *Nat. Rev. Microbiol. 7* (9), 629−641.

(3) Lewis, K. (2010) Persister cells. *Annu. Rev. Microbiol. 64* (1), 357−372.

(4) Keren, I., Kaldalu, N., Spoering, A., Wang, Y., and Lewis, K. (2004) Persister cells and tolerance to antimicrobials. *FEMS Microbiol. Lett. 230* (1), 13−18.

(5) Allison, K. R., Brynildsen, M. P., and Collins, J. J. (2011) Metabolite-enabled eradication of bacterial persisters by aminoglycosides. *Nature 473* (7346), 216−220.

(6) Conlon, B. P., Nakayasu, E. S., Fleck, L. E., LaFleur, M. D., Isabella, V. M., Coleman, K., Leonard, S. N., Smith, R. D., Adkins, J. N., and Lewis, K. (2013) Activated ClpP kills persisters and eradicates a chronic biofilm infection. *Nature 503* (7476), 365−370.

(7) Lehar, S. M., Pillow, T., Xu, M., Staben, L., Kajihara, K. K., Vandlen, R., DePalatis, L., Raab, H., Hazenbos, W. L., Morisaki, J. H., et al. (2015) Novel antibody-antibiotic conjugate eliminates intracellular *S. aureus*. *Nature 527* (7578), 323−328.

(8) Helaine, S., and Kugelberg, E. (2014) Bacterial persisters: formation, eradication, and experimental systems. *Trends Microbiol. 22* (7), 417−424.

(9) Beloin, C., Renard, S., Ghigo, J.-M., and Lebeaux, D. (2014) Novel approaches to combat bacterial biofilms. *Curr. Opin. Pharmacol. 18*, 61−68.

(10) Rajamuthiah, R., Fuchs, B. B., Jayamani, E., Kim, Y., Larkins-Ford, J., Conery, A., Ausubel, F. M., and Mylonakis, E. (2014) Whole animal automated platform for drug discovery against multi-drug resistant *Staphylococcus aureus*. *PLoS One 9* (2), e89189.

(11) Conery, A. L., Larkins-Ford, J., Ausubel, F. M., and Kirienko, N. V. (2014) High-throughput screening for novel anti-infectives using a *C. elegans* pathogenesis model. *Curr. Protoc. Chem. Biol. 6* (1), 25−37.

(12) Kim, W., Zhu, W., Hendricks, G. L., Van Tyne, D., Steele, A. D., Keohane, C. E., Fricke, N., Conery, A. L., Shen, S., Pan, W., et al. (2018) A new class of synthetic retinoid antibiotics effective against bacterial persisters. *Nature 556*, 103−107.



DOI: 10.1021/acsinfecdis.8b00161
*ACS Infect. Dis.* 2018, 4, 1540−1545

(13) Berger, J. P., Petro, A. E., Macnaul, K. L., Kelly, L. J., Zhang, B. B., Richards, K., Elbrecht, A., Johnson, B. A., Zhou, G., Doebber, T. W., et al. (2003) Distinct properties and advantages of a novel peroxisome proliferator-activated protein [gamma] selective modulator. *Mol. Endocrinol. 17* (4), 662−676.

(14) Li, Y., Yuan, H., von dem Bussche, A., Creighton, M., Hurt, R. H., Kane, A. B., and Gao, H. (2013) Graphene microsheets enter cells through spontaneous membrane penetration at edge asperities and corner sites. *Proc. Natl. Acad. Sci. U. S. A. 110* (30), 12295−12300.

(15) Wang, J., Wei, Y., Shi, X., and Gao, H. (2013) Cellular entry of graphene nanosheets: the role of thickness, oxidation and surface adsorption. *RSC Adv. 3* (36), 15776−15782.



DOI: 10.1021/acsinfecdis.8b00161
*ACS Infect. Dis.* 2018, 4, 1540−1545